Appl. Phys. B 67, 459–466 (1998)

Applied Physics B
Lasers
and Optics

CO-laser-based photoacoustic trace-gas detection: applications in postharvest physiology

J. Oomens[1,*], H. Zuckermann[2], S. Persijn[1], D.H. Parker[1], F.J.M. Harren[1]

[1] Department of Molecular and Laser Physics, University of Nijmegen, Toernooiveld 1, 6525ED Nijmegen, The Netherlands
(Fax: +31-24/365-3311, E-mail: Jos.Oomens@sci.kun.nl)
[2] Department of Exact and Life Sciences, Open University of Israel, 91904 Jerusalem, Israel

Received: 13 March 1998/Revised version: 13 May 1998

Abstract. A sensitive CO-laser-based photoacoustic trace-gas detector has been applied to study physiological processes in biological samples. A continuous flow-through system at atmospheric pressure leads the released trace gases from the sample to the photoacoustic resonator cells at flow rates where these processes can be studied with high time resolution. We focus here on transient effects that were found during fermentation of red bell peppers and apples, yielding in particular ethanol and acetaldehyde. Results are discussed also in the light of simultaneous O_2 measurements using polarographic oxygen sensors.

PACS: 42.55; 42.62; 82.80

Over the past years, laser-based photoacoustic (PA) trace-gas detection [1–3] has proven to provide a sensitive and non-intrusive method of studying physiological processes in biological samples. Using a photoacoustic cell placed inside a CO_2 laser cavity it became possible to detect the plant hormone ethylene (C_2H_4) at ppt[1] levels [4]. As ethylene plays an important role in several physiological processes in plants [5, 6], the applications are numerous: ripening of fruit [7], germination of seeds [8], pollination and wilting of flowers [9], flooding stress of *Rumex* plants [10] etc.

A CO-laser-based photoacoustic setup is well suited to detect a wide range of compounds important in biological research. Detection of ethanol and acetaldehyde is used to determine the rate of alcoholic fermentation in plant tissue during anoxic or hypoxic periods [11]. Ethane is detected as a tracer for cell membrane damage due to lipid peroxidation [12]. H_2O and CO_2 emissions are recorded to monitor breathing patterns of insects [13]. As one of the main contributors to the greenhouse effect, methane (CH_4) produced by bacteria present in, for example, rice paddies [14] and cockroaches [13] has been studied.

To further demonstrate the possibilities of this technique we report here on recent progress in the field of postharvest physiology. At present, worldwide postharvest losses, partly occurring in storage facilities, are estimated to amount up to 30% [15]. Monitoring metabolic responses of harvested crops is an asset in the development of new storage systems where the atmosphere is dynamically controlled based upon the levels of gaseous metabolites detected in the headspace [16].

Under normal aerobic conditions (21% O_2), crops produce energy by stepwise oxidation of glucose to the final products CO_2 and H_2O (respiration) [17]. In a nutshell, these steps include conversion of glucose to pyruvate, subsequent oxidation through the tricarboxylic acid (TCA) cycle to CO_2 and, finally, oxidative phosphorylation in which atmospheric O_2 is used to produce H_2O. Under anoxic conditions, an alternative process occurs to provide the energy required to sustain the life functions of the crop; pyruvate is now converted into acetaldehyde, which is quickly reduced to ethanol (fermentation). This latter pathway, however, renders far less energy per molecule of glucose than respiration. The 'lost energy' is actually trapped in ethanol – the end product of fermentation – and could only be released by further oxidation to water and CO_2 [17]. Schematically, the two processes can be summarized as follows:

Respiration:

$$\begin{aligned}&\text{Glucose} \rightarrow \text{pyruvate} \rightarrow \text{carbon dioxide and water}\\ &(C_6H_{12}O_6 \rightarrow C_3H_4O_3 \rightarrow CO_2 + H_2O)\end{aligned}$$

Alcoholic fermentation:

$$\begin{aligned}&\text{Glucose} \rightarrow \text{pyruvate} \rightarrow \text{acetaldehyde} \rightarrow \text{ethanol}\\ &(C_6H_{12}O_6 \rightarrow C_3H_4O_3 \rightarrow CH_3CHO \rightarrow C_2H_5OH)\end{aligned}$$

Alcoholic fermentation and respiration are not 'on/off' processes [18–20]; at low oxygen concentrations a fine balance exists between respiration and fermentation. As certain crops are transported and stored under low-oxygen conditions to slow down metabolic processes such as ripening, knowledge of the parameters determining the respiration-to-fermentation ratio is of crucial importance for the conservation of the product [16]. High levels of fermentative metabolites may affect firmness, flavor, and color of the crop.

* Corresponding author.

[1] 1 ppt = one part per trillion ($1 : 10^{12}$)

The effects of ethanol and acetaldehyde on plant tissue under oxygen deprivation have been widely studied [18]. The high reactivity of acetaldehyde is believed to cause cell death when present in relatively high amounts [21]. On the other hand, depending on the concentration, acetaldehyde is believed to inhibit ripening in some crops such as tomato [22] so that shelf life can be prolonged by exogeneously applying small amounts of this compound [23]. In other crops such as pear and blueberry, ripening is accelerated by acetaldehyde [22]. In addition, acetaldehyde is known to be one of the (many) components determining the flavor of most fruit [23].

When fermenting plant tissue is transferred from an anoxic to an aerobic atmosphere, an increase in the acetaldehyde emission occurs as a result of oxidation of ethanol accumulated in the tissue during the exposure to anoxia [24]. Due to the toxicity of acetaldehyde, this effect is believed to be the main cause for post-anoxic injury in plants rather than the high ethanol levels [21, 24, 25]. A recent study of the post-anoxic acetaldehyde upsurge in red bell pepper by Zuckermann et al. [11], showed that the peak in the emission occurs within less than 5 min after transfer to normoxic conditions. This extremely fast reaction has strengthened the belief that oxidation of ethanol by rapidly formed active oxygen species [26] such as hydrogen peroxide, stimulated by the enzyme catalase, is responsible for the acetaldehyde formation [11, 21].

1 Experimental methods

1.1 CO-*laser-based photoacoustic detection*

The CO laser and the resonant photoacoustic cells have been described in detail by Bijnen et al. [13, 27, 28]; here we give an overview focusing particularly on some recent developments. Three photoacoustic cells are placed inside the cavity of a liquid-nitrogen-cooled CO laser. The CO-laser frequency can be tuned over some 250 lines between 1300 and 2000 cm^{-1} [29], where most small-to-medium-sized molecules show strong and unique 'fingerprint' absorption features. By measuring the photoacoustic signals on several laser lines coinciding with absorption bands of different compounds and performing a least-squares multi-component analysis, concentrations of the different trace gases can be analysed simultaneously [1].

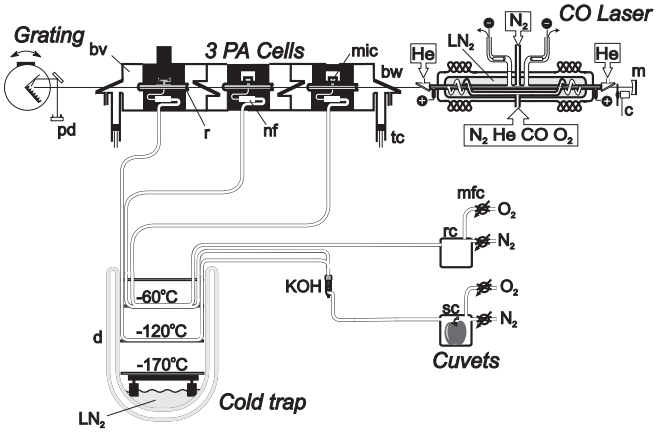

Fig. 1. Typical experimental setup as used for the bell pepper experiments. bv = buffer volume; bw = Brewster window; c = chopper; d = dewar; m = 100% mirror; mfc = mass flow controller; mic = microphone; nf = notch filter; pd = pyroelectric detector; r = resonator; rc = reference cuvette; sc = sample cuvette; tc = column of tunable length

Figure 1 schematically outlines the setup as used for fermentation experiments on bell peppers. The home-built CO laser consists of a Pyrex plasma tube (diameter 12 mm) surrounded by a liquid nitrogen reservoir. An outside vacuum jacket acts as thermal shielding to avoid condensation of water vapor on the laser and to reduce the liquid nitrogen consumption [29]. A continuous flow of helium, nitrogen, carbon monoxide, and air is led through the discharge tube at a pressure of about 25 mBar. The discharge is started by introducing a flow of N_2 between the two cathodes, which raises the ionization potential of the mixture at this point so that the two branches of the discharge are struck simultaneously [13]. To avoid deposition of particles from the plasma on the Brewster windows, a small He flow directed from each window towards the discharge is maintained.

The chopper frequency (≈ 1130 Hz) is optimized to match the resonance frequency of the resonators forming the heart of the PA cells. The resonance frequency of each cell can be finely adjusted individually by three heater elements. One of the cells is equipped with a sensitive condenser microphone (Brüel & Kjær 4179) and the other two with small – and less expensive – electret microphones (Knowles EK3024) [28]. Noise from the sample flow is reduced by notch filters on the cell inlet. To suppress contributions from absorptions by the ZnSe Brewster windows, buffer volumes and columns of tunable length are incorporated. Details on the effects of these elements are to be found in [13, 28].

The detection limits are mainly determined by the absorption coefficients of the trace gases on the different laser lines and by the intracavity laser power [13]. Interference by absorptions due to water may severely disturb the detection, as water is often released in large amounts by biological samples. To reduce the water concentration, the flow containing the trace gases is led over cold surfaces [27], the temperature of which can be set to values between 0 °C and −180 °C in order to trap out most of the water. In order to further reduce the water concentration and to avoid obstruction of the trap due to ice formation, the gas flow is dried using Nafion dryer tubings (Perma Pure Inc. Model MD-050) prior to entering the cold trap. A drawback of the Nafion tubing, however, is its tendency to trap other polar compounds such as ethanol. Not only does this effect cause a measured concentration up to about 20% lower than the actual concentration, it also leads to an increased ethanol background due to the slow release of ethanol from the Nafion tubing. No such effects were encountered for acetaldehyde. Different temperatures can be set for the flows leading to the three PA cells so that differential selection can be achieved, based on the differences in vapor pressure of trace gases under study [27]. After proper gas scrubbing practical (i.e. in a real multi-component sample) detection limits for the target gases typically reach ppb levels (see Table 1).

With the use of mass flow controllers (Brooks 5850), the O_2 concentration in the flow is accurately controlled, as was checked with a paramagnetic oxygen transducer (Servomex 1440) connected to the outlet of the PA cells. CO_2 produced by the sample is removed from the flow by a potassium hydroxide (KOH) scrubber to avoid both obstruction of the

Table 1. CO-laser lines and their absorption coefficients (in $atm^{-1}cm^{-1}$) for different trace gases[a] used in the experiments on red bell peppers. Note that the detection limits given here are practical limits as are reached in a realistic multi-component sample

Line $P(J'')_{v''}$	Freq./ cm^{-1}	$atm^{-1}cm^{-1}$ CH_3CHO	C_2H_5OH	C_2H_4	H_2O
$P(11)_{13}$	1765.46	**28.5**	0.028	0.0041	0.0093
$P(8)_{28}$	1406.91	6.07	**2.35**	0.31	0.0076
$P(11)_{26}$	1445.46	3.90	0.62	**1.02**	0.0075
$P(9)_{13}$	1772.89	14.2	0.018	0.0065	**1.37**
$P(11)_{24}$	1493.81	0.864	0.22	0.149	0.0133
Det. limit	(ppb)	0.5	10	10	10–100

[a] CH_3CHO = acetaldehyde; C_2H_5OH = ethanol; C_2H_4 = ethylene; H_2O = water

cold trap and possible spectral overlap with trace compounds under study. Part of the flow from the sample is cooled down to $-120\,^{\circ}C$ (see Fig. 1) to remove ethanol so that the much lower acetaldehyde concentrations can be determined independently [27]. In the flow over the $-60\,^{\circ}C$ surface, both ethanol and acetaldehyde are detected simultaneously.

The trace gas monitoring experiments are fully controlled by a personal computer (486 processor). The microphone signals from the PA cells are sampled by three lock-in amplifiers (Princeton Applied Research, one 5110 and two 5105s), which are connected to the computer through two RS232 serial ports. The PAR-5110 lock-in is equipped with two digital-to-analog converters (DACs) and four analog-to-digital converters (ADCs). The grating is rotated by a step motor (Oriel 18512) driven through two digital I/O channels of a Keithley PIO-12 interface. After a laser line has been selected with the step motor a piezo, mounted on the end mirror and controlled via one of the DACs of the PAR-5110 lock-in and a highvoltage amplifier, tunes the cavity over the gain profile. The power is monitored by a fast pyroelectric detector aligned to the zeroth-order reflection off the grating (see Fig. 1). A small electronic circuit rectifies and smooths the pyro signal which is then fed into the computer via one of the ADCs of the PAR-5110. Subsequently, the piezo voltage is reset to the value at which maximum power occurred. A more stable (though slower) value for the laser power, to normalize the measured PA signals, is obtained by demodulating part of the pyro signal using a lock-in amplifier (Ortec Brookdeal 9501E) with an RC time of typically 0.3 s. Signals from additional equipment, such as an infrared CO_2 analyzer (URAS, Hartmann & Braun) and mass flow controllers, can be read into the computer via the ADCs of the PAR-5110 or via a faster analog input board (Keithley DAS-801). In addition to the step motor, the digital I/O board controls eight valves which may be incorporated in the flow system. All software is written in C.

The procedure of positioning the laser and reading the PA signals, takes approximately one min per laser line. The liquid nitrogen level in the laser and in the cold trap are monitored with small molybdenum resistors that trigger electric valves to refill automatically when necessary. The temperatures of the different levels of the cold trap are actively stabilized using a temperature sensor and a heater element on each level.

In Table 1 absorption coefficients of acetaldehyde, ethanol, ethylene, and water are collected for the laser lines selected for the pepper experiments. The values in bold give the most prominent absorption features in the CO-laser range for each of the selected compounds. These coefficients were carefully calibrated using premixed samples with known concentrations of the volatiles in a buffer gas as will be detailed in a future publication [30]. As an example the absorption spectrum of ethanol in pure nitrogen at different CO-laser frequencies is shown in Fig. 2. The values are averaged over several runs and contributions from the background and remanent water in the PA cell are subtracted; the errors indicated represent one standard deviation. As each buffer gas (nitrogen or air) possesses different pressure broadening coefficients (see for example [31] for H_2O), it may slightly influence the absorption strength. In addition, the amount of water vapor in the buffer influences the vibration-to-translation relaxation rates of the gas sample [32] and thereby the phase of the photoacoustic signal [30].

For the detection of ethanol, a significant improvement has been achieved by including the $P(J'')_{v''} = P(8)_{28}$ laser line at $1406.9074\,cm^{-1}$. An absorption coefficient of $2.35\,atm^{-1}cm^{-1}$ is found on this relatively strong laser line [30, 33], which had not been recognized in previous studies [11, 27] and is a factor 2 to 3 higher than the coefficients on previously used laser lines. Note that the choice whether or not to include a certain laser line in the multi-line analysis is not solely based on the intensity of the absorption of a specific trace compound on that line. Other relevant criteria are a reasonable intracavity power and low interference with other compounds, especially with water.

In order to determine the concentrations of n substances, the photoacoustic signals on at least n laser lines must be recorded. Including more laser lines in one cycle does not necessarily improve the determination of concentrations. Of key importance is the orthogonality of the matrix $\vec{\vec{\Sigma}}$ containing the absorption coefficients Σ_{ij} of substance i on laser line j [2]. In other words, if the spectrum (on the selected laser lines) of one of the compounds is similar to a linear combination of spectra of the other compounds, concentrations cannot be well determined.

In order to check mutual interferences of the absorbing trace gases within the selected set of laser lines, the

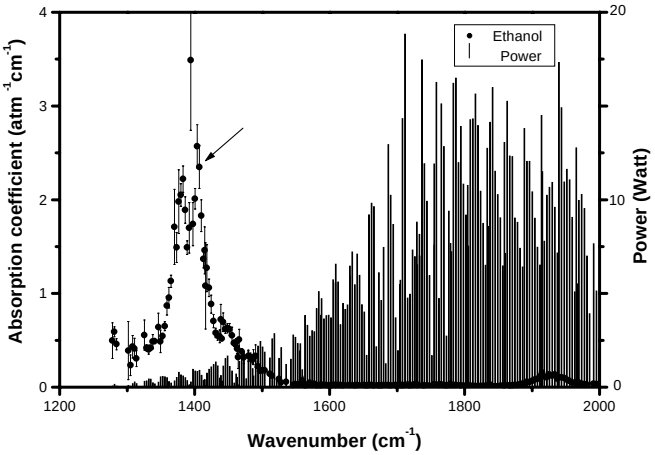

Fig. 2. Absorption coefficients of ethanol and intracavity laser power on the $\Delta v = 1$ CO-laser lines. The arrow indicates the $P(8)_{28}$ line used for ethanol detection

Table 2. Cross sensitivities [2] Q_{ij} for the selected set of laser lines and compounds to be detected

Line		Q_{ij}			
$P(J'')_{v''}$	$i\downarrow \quad j\rightarrow$	CH_3CHO	C_2H_5OH	C_2H_4	H_2O
$P(11)_{13}$	CH_3CHO	**1**	0.00098	0.00014	0.00033
$P(8)_{28}$	C_2H_5OH	2.7	**1**	0.14	0.0034
$P(11)_{26}$	C_2H_4	3.8	0.61	**1**	0.0074
$P(9)_{13}$	H_2O	10.4	0.013	0.0047	**1**

cross-sensitivities,

$$Q_{ij} = \frac{\Sigma_{ij}}{\Sigma_{ii}} , \tag{1}$$

as defined in [2], were evaluated (see Table 2). An error Δc_j in the concentration of compound j causes an error Δc_i in the concentration of compound i,

$$\Delta c_i \geq Q_{ij} \Delta c_j . \tag{2}$$

Most off-diagonal Q_{ij} values in Table 2 are relatively small, except for the values in the first column; an error in the acetaldehyde concentration thus causes a 2- to 10-fold higher error in the concentration of the other substances. However, acetaldehyde concentrations are usually several orders of magnitude lower than other concentrations (except for C_2H_4) and moreover, acetaldehyde concentrations are usually accurately determined due to the high contrast of its absorption spectrum. The interference between ethylene and ethanol also requires some caution; a high ethanol concentration, such as during fermentation, may cause a relatively large error in the C_2H_4 concentration (which is by the way very low for pepper [7]). It is noted however, that under anoxia, where the ethanol emission reaches a maximum, ethylene is not produced [6].

In practice, to determine the concentration of n substances, the PA signal on at least $n+1$ laser lines must be sampled (see Table 1) since background absorptions (cell windows, cell walls) give small contributions to the signal. Mathematically, the background can simply be treated as the $(n+1)$th compound to be detected.

The time required for a full measuring cycle should be short with respect to the time scale of the dynamic biological processes under study, so that concentrations in the PA cells do not significantly change during a cycle. In the experiments described here, a full cycle including five laser lines takes about five min. In contrast to some previous experiments [11, 27], we found that inclusion of more laser lines (up to 15) did not significantly improve the determination of trace-gas concentrations. This result is mainly based on the more accurately determined absorption coefficients [30] with respect to previous values [11, 27].

1.2 Oxygen measurements

Oxygen concentrations determine the balance between fermentation and respiration in the sample. Since oxygen possesses no infrared-active bands, it cannot be detected with the photoacoustic apparatus described here. A Clark-style polarographic sensor consisting of two electrodes (Pt and AgCl) in an electrolyte solution has been applied to determine the oxygen content inside bell peppers. If a voltage of about -0.7 V is applied to the electrode, the current is directly proportional to the O_2 concentration. As the current typically amounts to a few tenths of a nA, measurements were performed inside a metal box to shield the sensor from any unwanted electromagnetic radiation generated by other laboratory equipment.

Two different sensors were used; a microsensor built at the University of Amsterdam (NL) possessing a sharp (and fragile) glass tip [34] particularly suited for measurements with high spatial resolution, for example in sediments [35]. The second sensor, which is commercially available (Diamond General Corp. model 733), was equipped with a plastic cover to protect the glass tip containing the electrodes. The current from the electrodes was measured with a pA meter (Keithley) and read into a computer [36]. The performances of both sensors were comparable; a resolution of approximately 0.5% O_2 in the gas phase was reached. As spatial resolution was not required for the pepper measurements, the latter probe proved to be more practical in use due to its robustness.

The electric current in air and in pure nitrogen were measured to calibrate the sensor and a linear response was assumed for O_2 concentrations between 0 and 21%.

A hole (diameter 3 mm) was punctured through the skin of a pepper to insert the oxygen sensor into the locule. Using the Diamond General probe, the hole was then sealed with vacuum clay to avoid gas exchange through the hole. The pepper was placed in a cuvette which could be flushed with air or nitrogen. It has thus been possible to determine the time-dependent oxygen concentration inside the pepper at various external O_2 concentrations to derive the diffusion time of oxygen through the tissue.

2 Applications in postharvest physiology

Here we show recent results in the field of postharvest physiology of bell peppers and apples where the application of the PA detection technique has proven to be superior to conventional techniques. To better observe the dynamic behavior of the processes under study, each measurement was performed on a single piece of fruit to avoid smearing-out effects. It has not been our intention to give a full quantitative account of the physiological effects observed. Therefore, the data shown are in general obtained from a single sample and are not averaged over several replicates.

2.1 Oxygen diffusion and up-take in bell pepper

When the atmosphere surrounding a bell pepper is switched between anoxic and normoxic (and vice versa), the internal oxygen concentration follows an exponential build-up curve as shown in Fig. 3. For the pepper, the internal oxygen concentration is determined by diffusion and consumption. We assume that the diffusion flux (j_d) is proportional to the difference between internal and external partial oxygen pressures (p_{in} and p_{out}) and that the consumption flux (j_c) is proportional to the internal O_2 concentration so that

$$-\frac{dp_{in}}{dt} = j_d + j_c = \alpha(p_{in} - p_{out}) + \beta p_{in} . \tag{3}$$

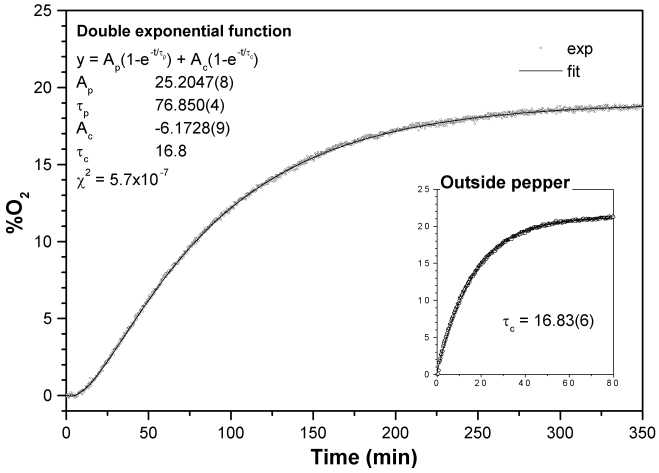

Fig. 3. Oxygen concentration inside a red bell pepper after switching from a nitrogen to an air flow at $t = 0$. The inset shows the same curve for an empty cuvette

The small onset visible between 0 and 10 min is due to the time required to fill the cuvette with air (partial oxygen pressure of p_{21}), which follows an exponential function

$$p_{\text{out}} = (1 - \mathrm{e}^{-t/\tau_c})\, p_{21} \tag{4}$$

that can be characterized by placing the oxygen sensor in the cuvette outside the pepper (see inset of Fig. 3). The parameters of this latter function depend on the volume of the cuvette and the flow rate. Under our conditions (935 ml cuvette, 2 l/h flow) a time constant of $\tau_c = 16.8$ min was found for the cuvette.

Inserting (4) into (3) yields an inhomogeneous differential equation

$$-\frac{\mathrm{d}p_{\text{in}}}{\mathrm{d}t} = \alpha[p_{\text{in}} - (1 - \mathrm{e}^{-t/\tau_c})\, p_{21}] + \beta p_{\text{in}}\,, \tag{5}$$

which, using the appropriate boundary conditions, has a solution in the form of a double exponential function

$$p_{\text{in}}(t) = A_{\text{p}}(1 - \mathrm{e}^{-t/\tau_{\text{p}}}) + A_{\text{c}}(1 - \mathrm{e}^{-t/\tau_{\text{c}}})\,, \tag{6}$$

where A_{p} and A_{c} have opposite signs and

$$\tau_{\text{p}} \equiv (\alpha + \beta)^{-1}\,, \tag{7}$$

$$-\frac{A_{\text{c}}}{A_{\text{p}}} = \frac{\tau_{\text{c}}}{\tau_{\text{p}}}\,, \tag{8}$$

$$|A_{\text{p}} + A_{\text{c}}| = \frac{\alpha}{\alpha + \beta}\; p_{21}\,. \tag{9}$$

A fit of the internal partial oxygen pressure of Fig. 3 to (6) yields $\tau_{\text{p}} = 76.9$ min as time constant for the pepper while the time constant for the cuvette is kept fixed to $\tau_{\text{c}} = 16.8$ min In addition, the fit yields $A_{\text{p}} = 25.2$ and $A_{\text{c}} = -6.2$ determining an internal oxygen concentration of 19.0% at $t = \infty$ which reflects the oxygen consumption due to respiration. On average, under normoxic conditions (21% O_2) an internal oxygen concentration of about 18% was found, in agreement with values found for some related species [37].

The assumption that the oxygen consumption is directly proportional to the internal oxygen concentration ($j_{\text{c}} = \beta p_{\text{in}}$) is not trivial since saturation effects may occur; however, from the fit presented in Fig. 3 we conclude that (6) represents an adequate description of the internal oxygen concentration.

2.2 Onset of fermentation in bell pepper

Dutch Red Bell Peppers (*Capsicuum annuum* cv. Presenta) with a typical fresh weight of 175 g were obtained from a local retailer during the months August – November 1997. Experiments were performed in an illuminated laboratory at room temperature.

Approximately 2 h after the transfer of red bell peppers from normoxic to anoxic conditions, the acetaldehyde level starts rising. Figure 4 shows that about 1 h later an intermediate plateau is reached during which the acetaldehyde emission remains at a constant level of about one fourth of the final level that is reached several h later. A similar effect has been observed for green bell peppers as shown in the inset of Fig. 4.

Acetaldehyde emissions from the pericarp (skin) and from the stem were recorded separately to investigate the influence of their different diffusion properties. To this end, a pepper was placed in a cuvette with two separate compartments; one of the compartments was placed over the stem site and sealed with vacuum clay and the other compartment collected trace gases emitted from the pericarp. Typically, the acetaldehyde emission from the pericarp starts one h earlier than the release from the stem (see Fig. 5), i.e. from the locule since we assume that the emission from the outside of the stem site is negligible. This delay is attributed to the concerted action of oxygen diffusion and consumption, causing the surface-near cells to be deprived of oxygen sooner than the more inner ones, which are fed by the oxygen inside the locule.

The contribution from the pericarp amounts to about 10% of the total acetaldehyde emission. For ethylene release, a pericarp–stem emission ratio of 25/75 has been found previously [7].

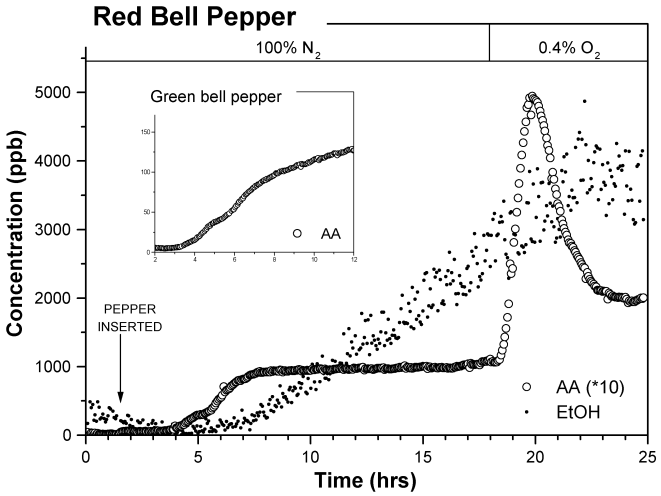

Fig. 4. Acetaldehyde and ethanol emission of one red bell pepper under anoxia. The pepper is inserted into the anoxic environment of the cuvette at $t = 1.5$ h. The plateau in the acetaldehyde emission (around $t = 5$ h) during the onset of fermentation is clearly visible. The inset shows the typical plateau as observed for a green bell pepper. Post-anoxic addition of only 0.4% O_2 leads to a dramatic increase of the acetaldehyde release within 20 min. (Note that the acetaldehyde concentration has been multiplied by 10 for clarity)

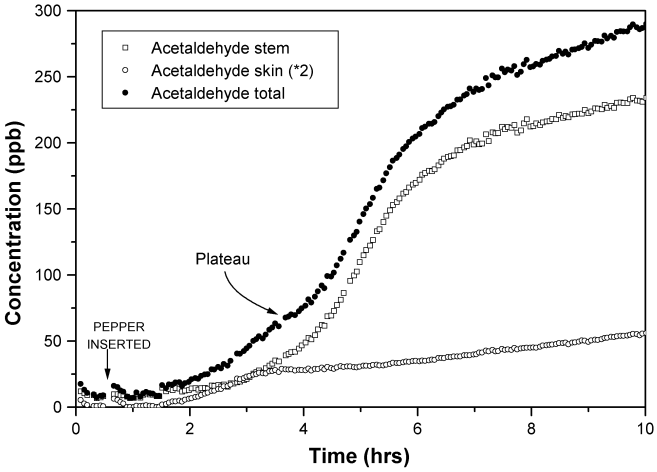

Fig. 5. Acetaldehyde emission of the stem and pericarp (skin) site recorded separately. The contribution from the pericarp has been multiplied by a factor of 2 for clarity. Summing both traces reveals the origin of the plateau during the onset of fermentation

Summing the acetaldehyde emissions from the stem and the pericarp indeed yields a plateau in the total release, at approximately one fifth of the final level. Thus, we conclude that the observed plateau originates from the hollow structure of a bell pepper and the differences in diffusion times through stem and pericarp. The 1-h delay between emission from the pericarp and from the locule (through the stem) corresponds well to the observed oxygen diffusion time. The times $\left(e^{-1}\right)$ required to adjust the concentration of N_2 in the cuvette and in the locule of the pepper differ by about 1 h.

Figure 4 also shows the ethanol release of the bell pepper which has been recorded simultanuously with the acetaldehyde release. Instead of reaching a steady production, a gradual increase is observed for at least 20 h and moreover, the production is an order of magnitude higher. The higher noise levels on the ethanol signals with respect to the acetaldehyde signals are attributed to: (i) the lower detection efficiency, (ii) stronger spectral overlap by water absorptions, (iii) higher temperature of the cold trap leading to higher concentrations of background gases, and (iv) partial trapping of ethanol by the Nafion tubing.

In addition, the ethylene release was monitored but no production was observed. Using a CO_2-laser-based PA detector, De Vries et al. [7] found a total production rate of 4 nl/h per fruit which corresponds to a concentration of about 1 ppb at a typical flow rate of 5 l/h. The practical detection limit for ethylene of our apparatus is estimated around 5 ppb. Moreover, it is known that oxygen is required to assimilate ethylene from its precursor ACC (1-aminocyclopropane-1-carboxylic acid) [6]. Under our low-oxygen conditions, the C_2H_4 production is probably even lower than the values reported in [7], depending on the ACC concentration [5, 6].

2.3 Post-anoxic acetaldehyde release

Zuckermann et al. studied the dynamics of the acetaldehyde release of red bell pepper upon transfer from an anoxic to a normoxic (21% O_2) atmosphere [11]. Here, we investigate the post-anoxic upsurge in acetaldehyde release as a function of the post-anoxic O_2 concentration.

Hereto, red bell peppers were placed in a cuvette connected to the PA system and a 5 l/h flow of pure nitrogen was supplied. The acetaldehyde release was monitored as the pepper was left anoxic overnight so that stable concentrations of typically 100 ppb were obtained, corresponding to a production of 500 nl/h per fruit. Then, the composition of the flow over the sample was changed to contain oxygen concentrations varying from 0.1% to 1.2%.

In all experiments a post-anoxic upsurge of acetaldehyde production was observed. The height of the peak amounted to approximately 4 times the level during fermentation under pure N_2. Comparing for example Fig. 4 with Fig. 3 of [11], one finds that the ratio of the post-anoxic peak to the anoxic level is hardly affected by the post-anoxic O_2 concentrations of 0.4% and 20%, respectively. However, the oxidation of ethanol occurs more slowly at lower O_2 concentrations as can be noticed by comparing the slope of the rising flank of the post-anoxic acetaldehyde peak. Table 3 summarizes peak heights and slopes for several post-anoxic oxygen concentrations. It may seem that for lower post-anoxic O_2 pressures the total amount of released acetaldehyde becomes larger; however, due to uncertainties regarding the decay of the post-anoxic upsurge, we refrain from such a conclusion.

As can be seen in Fig. 4, post-anoxic exposure to O_2 leaves the ethanol release rather unaffected. A decrease might be expected here to compensate for the ethanol being oxidized to acetaldehyde. However, as explained in [11], the lower detection efficiency and the 15-fold lower volatility of ethanol as compared to acetaldehyde [38], prevent observation of this effect.

An attempt was made to re-expose the fruit gradually to oxygen. The lowest O_2 concentration that could be reliably achieved by dynamically diluting air with pure nitrogen using two mass flow controllers was 0.05%. In Fig. 6, 0.05% O_2 was introduced after 8 h of anoxia leading to a 20% increase in acetaldehyde production in 1 h. Gradually increasing the oxygen content slowly *decreased* the acetaldehyde production even to below the anoxic level. Finally, switching the O_2 concentration abruptly to 20% yielded the well-known post-anoxic upsurge. This result may have important implications for common postharvest storage of fruit under low-oxygen conditions. Gradually restoring normal air conditions may reduce possible adverse effects [21, 24] of post-anoxic acetaldehyde emission.

As to the underlying processes causing the reduced post-anoxic acetaldehyde release, no previous studies are known to us so that we can only give some preliminary thoughts here.

Table 3. Post-anoxic acetaldehyde peak height (relative to anoxic acetaldehyde level) and slope of the rising flank for various post-anoxic oxygen concentrations applied to fermenting red bell peppers. The slope gives the increase (per hour) in production normalized for the fresh weight of the sample (nl/gFWh)

$[O_2]$ (%)	Peak (ratio)	Slope/ nl/gFWh^2
0.1	3.8	4.9
0.2	3.5	5.6
0.4	4.7	12.7
1.2	3.6	18.8
20.0	3.8	38.1

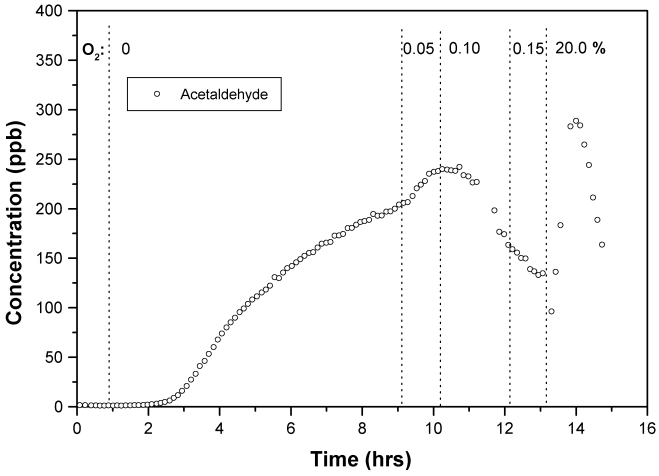

Fig. 6. Post-anoxic acetaldehyde emission is reduced (compare to Fig. 4) by gradually restoring the oxygen content. A sudden increase to 20% yields the known effect

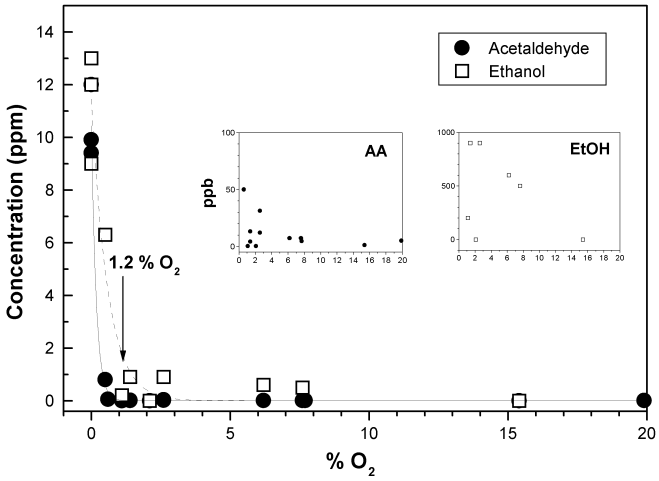

Fig. 7. Ethanol and acetaldehyde production of apples as function of the external oxygen concentration. A zoom of the emissions for O_2 concentrations above 1% is shown in the insets

The amount of post-anoxic acetaldehyde depends (partly) upon the production rate of active oxygen species (AOS), which depends on the O_2 concentration, and (partly) upon the availability of the substrate, ethanol, which decreases at higher O_2 concentrations due to the restoration of normal respiration. Thus, upon re-exposure to oxygen, ethanol oxidation and oxidative phosphorylation compete for the available O_2 molecules. Additionally, the availability of AOS scavenging enzymes (such as superoxide dismutases [26]) and normal respiration enzymes plays an important role. More detailed studies are necessary to clarify the observations.

2.4 Fermentation vs. O_2 *concentration for apples*

Apples (*Malus domestica* Borkh., cv. Elstar) were harvested in September 1995 whereafter they were stored under controlled atmosphere (1 °C, 1.2% O_2, and 0.5% CO_2) for three months. The apples were then put in air-tight bottles connected to a flow-through system and supplied with various partial oxygen pressures for about five days. One by one, the bottles containing the apples under different oxygen concentrations were connected to the flow system of the PA detector. Flushing the bottles with 0.5 l/h of pure nitrogen, the ethanol and acetaldehyde concentrations in the headspace were analysed. A stable value was obtained after about half an hour.

Figure 7 depicts the production rate of the fermentative metabolites as a function of the applied oxygen concentration. Even at higher O_2 concentrations, ethanol and acetaldehyde production is observed suggesting that fermentation is still active though at a low rate (see inset). The critical oxygen concentration, where respiration turns to fermentation, is located around 1.2% as seen from the plot [20]. Note that the internal concentration is much lower due to the resistance to diffusion of the tissue [39].

Although the acetaldehyde concentration is typically an order of magnitude lower than the ethanol concentration, it shows a much sharper response to the onset of fermentation as observed for both apples and bell peppers. The higher vapor pressure for acetaldehyde with respect to ethanol is the most obvious explanation for this observation. For monitoring purposes during controlled-atmosphere crop storage, acetaldehyde may therefore serve as an accurate indicator for fermentation. The more gentle slope of the ethanol vs. oxygen curve suggests the existence of memory effects in the tissue which may mask the true physiological state of the fruit and lead to erronous decisions during storage.

The measured release of acetaldehyde and ethanol was used to model the fermentative CO_2 production [17] as a function of the oxygen concentration during storage of apples. A detailed analysis has been presented by Peppelenbos et al. [20].

3 Conclusions

Fast physiological processes or responses justify the application of trace detectors featuring a high time resolution. To understand these processes in detail it is necessary to study a single piece of fruit to avoid averaging out of the transient effects. Thus, the detector to be applied should not only possess a high time resolution but also a high sensitivity. We have shown that an intracavity CO-laser-based photoacoustic detector combined with a continuous flow-through system satisfies these requirements. Conventional techniques with high sensitivity such as gas chromatography often fail to register the transient effects due to long accumulation times.

Compared to previous studies applying the same apparatus [11, 27] it has been possible to reduce the time resolution from about 15 to 5 min by reducing the number of laser lines sampled in one cycle, without a significant loss of information; an accurate calibration of absorption coefficients allows one to record the PA signals on the minimum number of laser lines $(n+1)$ needed for the simultaneous detection of a certain number (n) of trace compounds. For ethanol detection a significant improvement was achieved thanks to the introduction of the $P(8)_{28}$ laser line where a more than twice higher absorption coefficient was found compared to [11, 27].

A time resolution of around 10 s was obtained by Bijnen et al. [13] measuring the PA signal on a single laser line to study breathing patterns of cockroaches and of several other insects. This extremely fast technique did not allow the monitoring of more than one trace-gas concentration at the same

time and additionally, one had to rely on a constant concentration of background gases. Here, we have presented a practical compromise; by scanning over five laser lines four different trace concentrations have been analysed simultaneously with a reasonable time response.

From a plant physiological point of view, we found that for bell pepper the post-anoxic O_2 concentration determines the rate of ethanol oxidation, but does not affect the acetaldehyde peak value. Furthermore, it has been possible to reduce the post-anoxic acetaldehyde release by gradual restoration of an aerobic atmosphere. Transient effects in the acetaldehyde release during the onset of fermentation have been shown to be diffusion related. For apples, the ethanol and acetaldehyde emissions as a function of the external oxygen concentration have been compared.

Acknowledgements. It is a pleasure to acknowledge the excellent technical support of C. Sikkens, C. Timmer, and H. Schoutissen. We greatly enjoyed the numerous discussions with Prof. J. Reuss and Dr. H. de Vries. We thank Dr. H.W. Peppelenbos for proofreading the manuscript and Dr. B. de Winder for lending us the oxygen microsensors and additional equipment. This research is supported by the Technology Foundation STW, Applied Science division of NWO and the Technology programme of the Ministry of Economic Affairs.

References

1. S. Bernegger, M.W. Sigrist: Infrared Phys. **30**, 375 (1990)
2. P.L. Meyer, M.W. Sigrist: Rev. Sci. Instrum. **61**, 1779 (1990)
3. F. Harren, J. Reuss: In *Encyclopedia of Applied Physics, Vol. 19*, ed. by G.L. Trigg (VHC, New York 1997) pp. 413
4. H.S.M. De Vries, F.J.M. Harren, L.A.C.J. Voesenek, C.W.P.M. Blom, E.J. Woltering, H. van der Valk, J. Reuss: Plant Physiol. **107**, 1371 (1995)
5. S.F. Yang, N.E. Hoffman: Annu. Rev. Plant Physiol. **35**, 155 (1984)
6. F.B. Abeles, P.W. Morgan, M.E. Saltveit: *Ethylene in Plant Biology*, 2nd edn. (Academic Press, San Diego, CA 1973)
7. H.S.M. de Vries, M.A.J. Wasono, F.J.M. Harren, E.J. Woltering, H.C.P. M. van der Valk, J. Reuss: Postharvest Biol. Technol. **8**, 1 (1996)
8. L. Petruzzelli, F. Harren, J. Reuss: Environ. Exp. Bot. **34**, 55 (1994)
9. E.J. Woltering, F. Harren, H.A.M. Boerrigter: Plant Physiol. **88**, 506 (1988)
10. F.J.M. Harren, F.G.C. Bijnen, J. Reuss, L.A.C.J. Voesenek, C.W.P.M. Blom: Appl. Phys. B**50**, 137 (1990)
11. H. Zuckermann, F.J.M. Harren, J. Reuss, D.H. Parker: Plant Physiol. **113**, 925 (1997)
12. A.A.E. Martis, S. Büscher, F. Kühnemann, W. Urban: Instrum. Sci. Technol. **26**, 177 (1998)
13. F.G.C. Bijnen, F.J.M. Harren, J.H.P. Hackstein, J. Reuss: Appl. Opt. **35**, 5357 (1996)
14. F. Rothfuss, F.G.C. Bijnen, R. Conrad, F.J.M. Harren, J. Reuss: Chemosphere **33**, 2487 (1996)
15. T.C. Lioutas: Food Techn. **42**, 78 (1988)
16. S.P. Schouten, R.K. Prange, J. Verschoor, T.R. Lammers, J. Oosterhaven: Proc. 7th Int. Res. Conf. Contr. Atm. Stor., Davis, USA, **2**, 71 (1997)
17. See for example J.L. Gould, W.T. Keeton: *Biological Science*, 6th edn. (Norton, New York 1967) pp. 153; F.B. Salisbury, C.W. Ross: *Plant Physiology*, 4th edn. (Wadsworth, Belmont, CA 1992) pp. 266
18. M. Knee: In *Plant Life Under Oxygen Deprivation; Ecology, Physiology and Biochemistry*, ed. by M.B. Jackson, D.D. Davies, H. Lambers (SPB, The Hague 1991) pp. 229
19. B. Ricard, I. Couée, P. Raymond, P.H. Saglio, V. Saint-Ges, A. Pradet: Plant Physiol. Biochem. **32**, 1 (1994)
20. H.W. Peppelenbos, H. Zuckermann, S.A. Robat: Proc. 7th Int. Res. Conf. Contr. Atm. Stor., Davis, USA, **2**, 168 (1997)
21. L.S. Monk, R. Braendle, R.M.M. Crawford: J. Exp. Bot. **38**, 233 (1987)
22. J.C. Beaulieu, G. Peiser, M.E. Saltveit: Plant Physiol. **113**, 431 (1997)
23. E. Pesis, R. Marinansky: J. Plant Physiol. **142**, 717 (1993)
24. P. Perata, A. Alpi: Plant Physiol. **95**, 748 (1991)
25. M.B. Jackson, B. Herman, A. Goodenough: Plant Cell Environ. **5**, 163 (1982)
26. J.G. Scandalios: Plant Physiol. **101**, 7 (1993)
27. F.G.C. Bijnen, H. Zuckermann, F.J.M. Harren, J. Reuss: Appl. Opt. **37**, 3345 (1998)
28. F.G.C. Bijnen, J. Reuss, F.J.M. Harren: Rev. Sci. Instrum. **67**, 2914 (1996)
29. W. Urban: Infrared Phys. Technol. **36**, 465 (1995)
30. S. Persijn et al.: in preparation
31. T. Giesen, R. Schieder, G. Winnewisser, K.M.T. Yamada: J. Mol. Spectrosc. **153**, 406 (1992)
32. A.D. Wood, M. Camac, E.T. Gerry: Appl. Opt. **10**, 1877 (1971)
33. J. Oomens, S. Persijn, R.H. Veltman, A.C.R. van Schaik, H.S.M. de Vries, F.J.M. Harren, D.H. Parker: In *Chemical, Biochemical and Environmental Fiber Sensors IX*, ed. by R.A. Lieberman, Proc. SPIE **3105**, 387 (1997)
34. N.P. Revsbech: Limnol. Oceanogr. **34**, 474 (1989) and references therein
35. N.P. Revsbech, B.B. Jørgensen: Limnol. Oceanogr. **28**, 749 (1983); J.K. Gundersen, B.B. Jørgensen: Nature **345**, 604 (1990)
36. Z. Dubinsky, P.G. Falkowsky, A.F. Post, U.M. van Hes: J. Plankton Res. **9**, 607 (1987)
37. M.M. Blanke, P.A. Holthe: J. Plant Physiol. **150**, 247 (1996)
38. T.W. Kimmerer, R.C. MacDonald: Plant Physiol. **84**, 1204 (1987)
39. M.L. Tucker, G.G. Laties: Plant Cell Environm. **8**, 117 (1985)